Materials Science in Semiconductor Processing 39 (2015) 781–785

Contents lists available at ScienceDirect

Materials Science in Semiconductor Processing

journal homepage: www.elsevier.com/locate/matsci

Band gap engineering of CuS nanoparticles for artificial photosynthesis

K.R. Nemade [a,*], S.A. Waghuley [b]

[a] Department of Physics, Indira College, Kalamb 445401, India
[b] Department of Physics, Sant Gadge Baba Amravati University, Amravati 444602, India

ARTICLE INFO

Article history:
Received 30 January 2015
Received in revised form
23 May 2015
Accepted 23 May 2015

Keywords:
Nanostructures
Optical materials
Optical properties
Raman spectroscopy

ABSTRACT

CuS nanoparticles with engineered optical band gap that varies with substrate temperature were prepared by spray-pyrolysis technique. Structural, morphological, and optical characterization of the as-synthesized CuS nanoparticles was done through X-ray diffraction, field-emission scanning electron microscopy, Raman spectroscopy, photoluminescence spectroscopy, and ultraviolet–visible spectroscopy. This work provides a convenient method of tuning of the band gap for particular applications. We tuned the band gap of the as-synthesized CuS nanoparticles to fall within the wavelength range of 325–350 nm. We propose their use as light harvesting antenna in artificial photosynthesis.

1. Introduction

Copper sulfide (CuS) is wide-band-gap p-type semiconductor material with modern applications ranging from industrial to biomedical [1]. CuS nanoparticles have attracted increasing attention because of their various applications such those in as photothermal therapy [2], sensors [3], solar cells [4], catalysts [5], and hydrogel systems [6].

Artificial photosynthesis can provide a solution for reducing carbon dioxide (CO_2) into solar fuels. In the near future, this endeavor will be of great interest. Singh et al. reported the artificial photosynthesis by a novel composite photocatalyst based on TiO_2 and copper indium sulfide nanocrystals. These nanoparticles very high efficiency in using ultraviolet radiation in concentrated sunlight to convert fuels (4.3%) compared with that of platinum-doped TiO_2 nanoparticles (2.1%) [7]. Wendell et al. used a cell-free, artificial photosynthetic platform, which couples the requisite enzymes of the Calvin cycle with a nanoscale photophosphorylation system. This work reported significant efficiencies for chemical conversion, specifically, in carbon fixation and sugar synthesis using chemical energy [8]. Motivated by this work, we attempted to use CuS nanoparticles in light harvesting antenna in artificial photosynthesis.

Bulk CuS with hexagonal wurtzite structure has a direct band gap of ~2.5 eV [9]. Many studies have shown that the optical absorption CuS nanoparticles falls within a wide range (350–800 nm). Saranya et al. synthesized CuS nanoparticles by the hydrothermal route and analyzed their optical properties. They engineered the band gap of CuS to cover the range of 1.641–1.653 eV [10].

The literature on materials science described many approach to the synthesis of CuS nanostructures. Mathew et al. reported the synthesis of CuS nanoparticles through the photochemical method. They established the correlation between the amount of particles and the time of irradiation [11]. Krishnamoorthy et al. demonstrated the synthesis of CuS nanoparticles for supercapacitor applications through a one-pot hydrothermal approach [12]. Liu et al. synthesized cysteine-coated CuS nanoparticles with high photothermal conversion efficiency for cancer therapy. Their nanoparticles have photothermal conversion efficiency of ~38.0%, which is much higher than that reported in the literature [13]. Raevskaya et al. synthesized nanosized colloidal CuS particles by using indirect synthesis of CuS from CdS nanoparticles. The particles exhibit the quantum confinement effect, and their band gap is dependent on particles size [14].

Drawing from the research of Raevskaya et al. on band-gap reduction, we studied the band-gap engineering of CuS nanoparticles by using spray-pyrolysis technique at various temperatures. Band-gap engineering of nanoparticles has wide-ranging applications in fabrication of building blocks for various optoelectronic devices [15,16]. In the present work, we uased CuS nanoparticles in light-harvesting antenna in artificial photosynthesis.

Nanostructures in artificial photosynthesis enable fundamental processes that occurs in natural photosynthesis, one of which is light harvesting. Synthesis of such nanoparticles has only recently been possible because breakthroughs in nanotechnology. Therefore, we prepared nanoparticles that absorb in the ultraviolet-A

* Corresponding author.
E-mail address: krnemade@gmail.com (K.R. Nemade).

http://dx.doi.org/10.1016/j.mssp.2015.05.045
1369-8001/

region. The band gap of our nanoparticles could be tuned to within the range of 325–350 nm.

2. Experimental

2.1. Sample preparation

The CuS nanoparticles were synthesized by flame-assisted spray pyrolysis technique. Reagents used in this work, such as $Cu(NO_3)_2 \cdot 3H_2O$ and Na_2S, were of analytical grade. They were purchased from the commercial market and used without further purification. In the synthesis of CuS nanoparticles, 1 M solutions of $Cu(NO_3)_2 \cdot 3H_2O$ and Na_2S in distilled water of resistivity near to 20 MΩ cm were prepared separately. The prepared solutions were mixed rapidly by magnetic stirring for 30 min at room temperature. Subsequently, the final solution was placed in an ultrasonic homogenizer for 2 h. This solution was then loaded in a spray-pyrolysis chamber. Specifications of the spray-pyrolysis setup are described in a previous report [17]. In the present work, CuS nanoparticles were collected on chemically cleaned SiO_2 substrate. It is well known that the band gap is directly related to the average crystallite size and that the average crystallite size is temperature-sensitive. With these considerations in mind, we prepared the samples by varying the substrate temperature from 150–300 °C at 50 °C intervals. The heating platform in the spray-pyrolysis setup was used to maintain the temperature during spray-coating of substrates for 2 h.

2.2. Characterization

The structure and phase purity of CuS nanoparticles were examined by X-ray diffraction (XRD) analysis using Cu Kα radiation (Rigaku Miniflex-II; $\lambda = 1.5406$ Å). The surface morphology was investigated by field-emission scanning electron microscopy (FE-SEM) using JEOL JSM-7500F. The optical properties of the as-synthesized nanoparticles at room temperature were ascertained by using a Lambda 850 ultraviolet–visible spectrophotometer of (Perkin Elmer). Raman spectra of CuS nanoparticles were recorded on a Bruker spectrometer (2 mW laser power, 523 nm wavelength), and fluorescence spectra of samples was acquired on a fluorescence spectrophotometer (Hitachi F-7000).

3. Results and discussion

3.1. XRD experiments

XRD was used to characterize the phase purity and crystallinity of CuS nanoparticles synthesized by spray pyrolysis (results are shown in Fig. 1). Diffraction peaks at 2θ values could be perfectly indexed to the hexagonal phase of CuS with the corresponding cell parameters ($a = 3.7920$ Å, $b = 3.7920$ Å, $c = 16.3440$ Å; $P6_3/mmc$ space group) [18,19]. Diffraction peaks in the pattern could be exactly indexed to JCPDS Card No. 06-0464. The strong and sharp diffraction peaks show that the degree of crystallization increased with the processing temperature. The hypothesis for the mechanism of CuO formation from CuS nanoparticles at elevated temperature was proposed by Mu et al. [20]. According to this hypothesis, CuO forms by CuS oxidation. Therefore, some weak peaks in our case at around (101) and (006) may be ascribed to CuO formation on the CuS surface. The average crystallite size of the as-synthesized CuS nanoparticles was computed from the XRD pattern through the Debye–Scherrer equation [21], $D = (K\lambda/\beta \cos\theta)$, where D is average crystallite size (nm), K is a shape factor ($K = 0.89$), λ is the wavelength of the X-ray source (1.540 Å), β is the full width at half maximum, and θ is the diffraction peak angle. The width of the Bragg peak results from both instrument- and sample-dependent effects. To cancel these unwanted effects, obtaining the XRD pattern from the line broadening of a reference material (silicon) is essential to compute instrumental broadening. In this manner, instrument-corrected broadening (β) corresponding to CuS nanoparticles may by estimated by using Eq. (1),

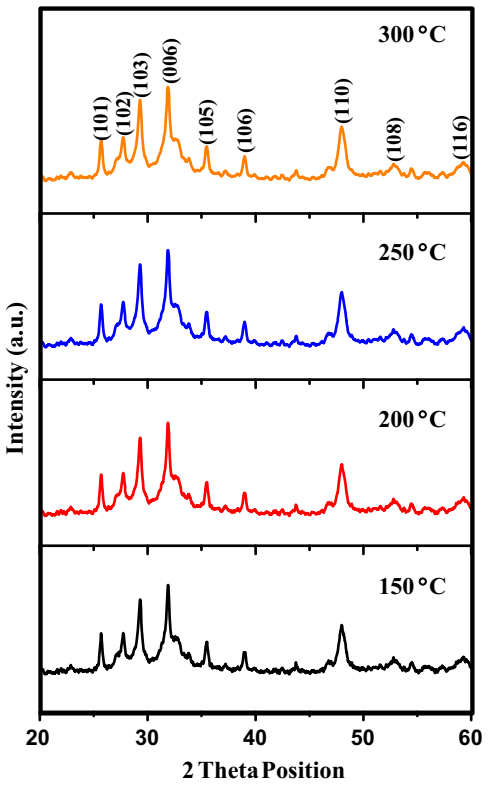

Fig. 1. XRD pattern of CuS nanoparticles deposited at various substrate temperatures.

$$\beta^2 = (\beta)^2_{measured} - (\beta)^2_{\text{int } rumental} \quad (1)$$

The average crystallite size, which was calculated by nullifying line broadening due to the equipment was in the range of 21.3–37.5 nm.

3.2. FE-SEM

The morphology of the products was examined by FE-SEM. FE-SEM micrographs of the samples at various substrate temperatures are shown in Fig. 2. The FE-SEM image of the obtained samples consisted of particles with various sizes. Careful inspection of the SEM images at constant magnification shows that the average crystallite size increases with the increase in substrate temperature. This insignificant variation in average crystallite size may be due to the heating process, which causes collision of particle, which then combine with to form larger particles. Particles combination is highly sensitive to the process temperature during the synthesis [22,23]. In our case, it was difficult to distinguish the direct effect of temperature on the average crystallite size possibly because of the small interval of temperature and heating period.

3.3. Raman spectroscopy

The effect of temperature on lattice vibrations of CuS was studied by Raman spectroscopy. The Raman spectrum of CuS nanoparticles at 150–300 °C were obtained. Raman spectra of CuS

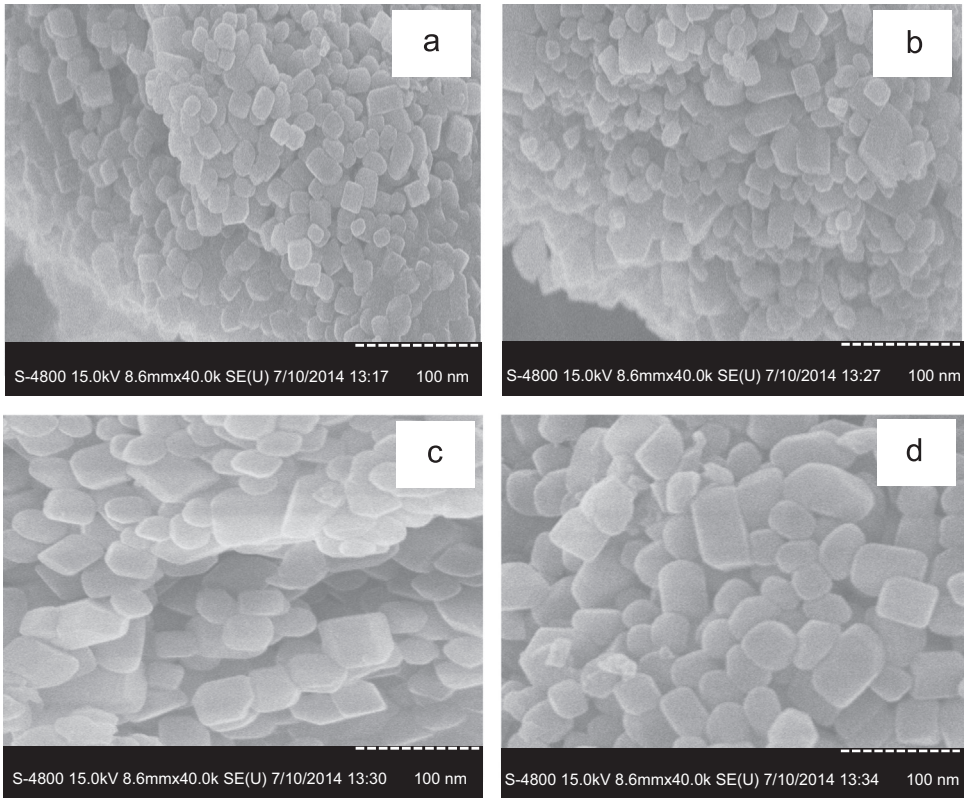

Fig. 2. FE-SEM images of CuS nanoparticles deposited at varous temperatures: (a) 150, (b) 200, (c) 250, and (d) 300 °C.

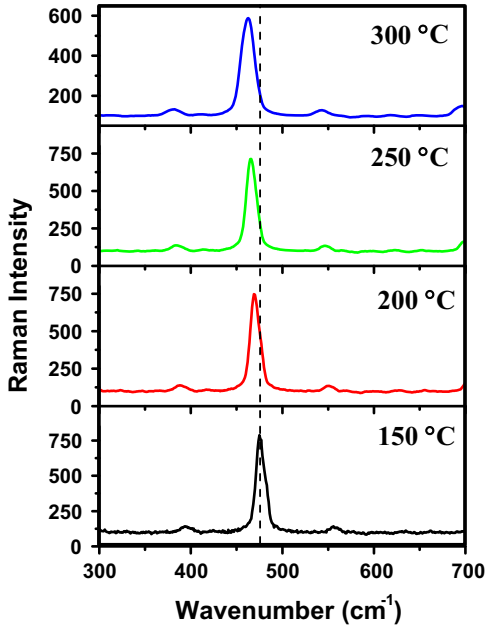

Fig. 3. Raman spectrum of CuS nanoparticles deposited at various substrate temperatures. The dashed arrow is used to depicts the variations of the peak position.

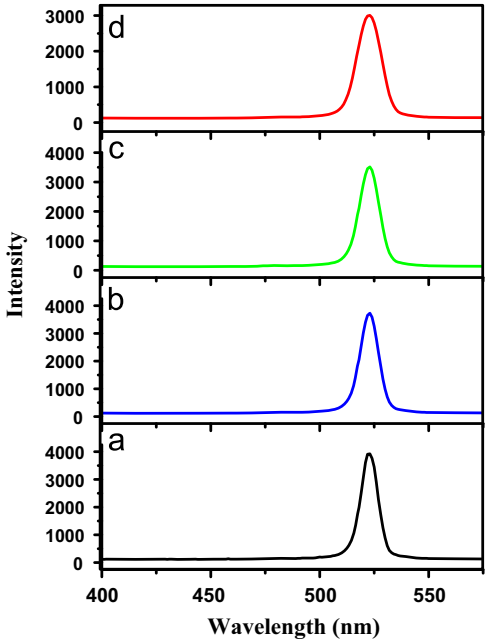

Fig. 4. Photoluminescence spectra of the CuS nanoparticles deposited at various temperature: (a) 150, (b) 200, (c) 250, and (d) 300 °C.

nanoparticles deposited at various temperatures are depicted in Fig. 3. A strong band at 472 cm^{-1} apparently originates from the lattice vibration of CuS [24]. The phonon frequency linearly decreased with increasing temperature, which could be directly observed by the shifting of characteristic peak of CuS toward lower wavenumbers. This decrease may be attributed to the vibration anharmonicity due to the effects of thermal expansion [25,26].

3.4. Photoluminescence (PL) measurement

The PL spectrum of CuS nanoparticles deposited at various substrate temperatures under excitation at 380 nm is shown in Fig. 4. The PL spectrum of nanoparticles exhibits strong emission at ~522 nm. This result differs from that of other studies on CuS nanoparticle, which report that PL is sensitive to particle shape [27]. In our case, CuS nanorystals acquired a nearly cubic shape.

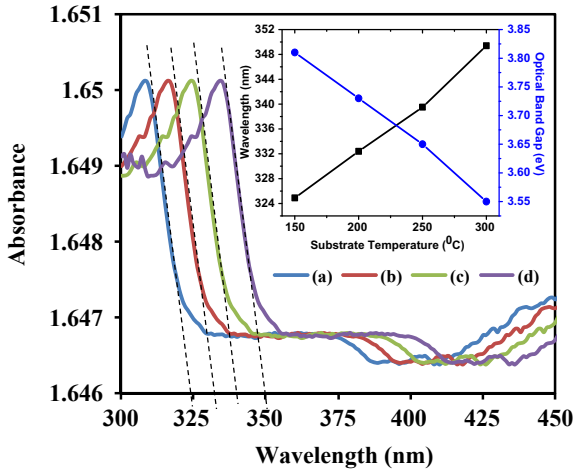

Fig. 5. UV–visible absorption spectra of CuS nanoparticles synthesized at substrate temperatures pf (a) 150, (b) 200, (c) 250, and (d) 300 °C. Inset shows the variation of band gap with substrate temperature.

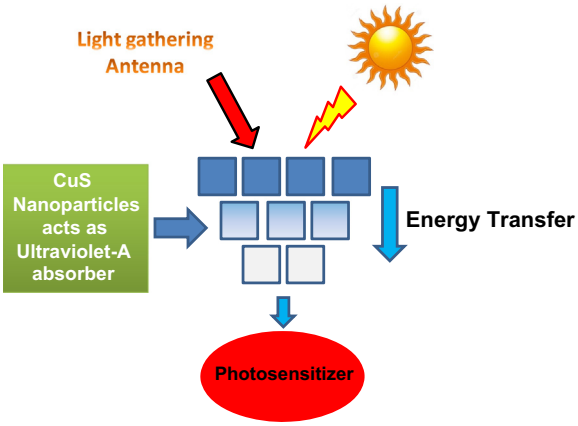

Fig. 6. Plausible application of the as-synthesized CuS nanoparticles as a light harvesting antenna in a leaf for artificial photosynthesis.

When the temperature increased from 150 to 300 °C, the full width of the peak at half maximum increased slightly. This is attributed to thermally active, phonon-assisted tunneling [28,29].

3.5. Optical band-gap measurement

Light harvesting requires absorption of ultraviolet A (UV-A) (3.10–3.94 eV) wavelength in the range of 325–350 nm. To analyze the optical properties of the as-synthesized CuS nanoparticles, the optical absorption of the samples were in the wavelength range of 300–450 nm, as shown in Fig. 5. The absorption wavelength was determined by extrapolating the line to the linear region of the absorbance spectrum. The optical band gap of the sample was estimated by using the energy–wavelength relation, $Eg = hc/\lambda$, where h is the Plank's constant, c is the velocity of light and λ is the wavelength determined from absorption tail.

Close observation of absorption spectra of the CuS nanoparticles directly shows that with increasing substrate temperature, absorption tail shifts toward longer wavelength (red shift). The optical band gap of the as-synthesized materials redshifted, whereas PL measurements blueshifted. This may be due to quantum trapping and electron–phonon coupling in the atomic layers of the surface. In this process, materials in the interior retain their bulk nature. The extent of blue- and redshifting in the sample depends on the tunable fraction of undercoordinated atoms on the surface skin. Thus, the quantum confinement effect is present on the surface that is superficial in nature[30].

The inset of Fig. 5 shows that the band gap of the samples increased with the increase in substrate temperature. According to the hyperbolic band model [31] and effective mass approximation [32], the optical band gap and particles size are inversely related. SEM results related to the average crystallite size are in good agreement with those from UV–visible absorption spectroscopy.

In the present work, the absorption wavelength of as-synthesized samples were found to be in the range of 325–350 nm, which corresponds to the UV-A range (3.10–3.94 eV). This region plays an important role in photosynthesis in plants. A possible application of the as-synthesized CuS nanoparticles is described in Fig. 6. The nanoparticles may be used as light-harvesting antenna for energy transfer toward the photosensitizer [33].

4. Conclusions

In summary, we synthesized CuS nanoparticles by spray-pyrolysis technique. XRD analysis showed the phase and structural purity of CuS nanoparticles. SEM indicated that the average crystallite size is affected by substrate temperature. Similarly, PL and Raman analysis showed that substrate temperature affects average crystallite size and lattice vibration. The band gap of prepared nanoparticles was found to be a function of substrate temperature. CuS nanoparticles deposited at various substrate temperatures exhibited absorption tail in the wavelength range of 325–350 nm. Therefore, we propose the use of the prepared nanoparticles in the light-harvesting antenna in artificial photosynthesis.

Acknowledgments

The authors thank Prof. S.K. Omanwar, head of the Department of Physics, Sant Gadge Baba Amravati University, Amravati, for providing the necessary facilities for this work.

References

[1] A.A. Sagade, R. Sharma, Sens. Actuators B 133 (2008) 135–143.
[2] Q. Tian, F. Jiang, R. Zou, Q. Liu, Z. Chen, M. Zhu, S. Yang, J. Wang, J. Wang, J. Hu, ACS Nano 5 (2011) 9761–9771.
[3] L. Qian, J. Mao, X. Tian, H. Yuan, D. Xiao, Sens. Actuators 176 (2013) 952–959.
[4] Y. Wu, C. Wadia, W. Ma, B. Sadtler, A.P. Alivisatos, Nano Lett. 8 (2008) 2551–2555.
[5] Z. Peralta-Inga, P. Lane, J.S. Murray, S. Boyd, M.E. Grice, C.J. Oconnor, P. Politzer, Nano Lett. 3 (2003) 21–28.
[6] C. Tan, Y. Zhu, R. Lu, P. Xuea, C. Bao, X. Liu, Z. Fei, Y. Zhao, 91 (2005) 44–47.
[7] V. Singh, I.J.C. Beltran, J.C. Ribot, P. Nagpal, Nano Lett. 14 (2014) 597–603.
[8] D. Wendell, J. Todd, C. Montemagno, Nano Lett. 10 (9) (2010) 3231–3236.
[9] R.S. Christy, J.T.T. Kumaran, J. Non Oxide, Glass 6 (2014) 13–22.
[10] M. Saranya, C. Santhosh, R. Ramachandran, A.N. Grace, J. Nanotechnol. 2014 (2014) 321571–321579.
[11] S.K. Mathew, N.P. Rajesh, M. Ichimura, M. Udayalakshmic, Mater. Lett. 62 (2008) 591–593.
[12] K. Krishnamoorthy, G.K. Veerasubramani, A.N. Rao, S.J. Kim, Mater. Res. Express 1 (2014) 035006–035014.
[13] X. Liu, B. Li, F. Fu, K. Xu, R. Zou, Q. Wang, B. Zhang, Z. Chen, J. Hu, Dalton Trans. 14 (2014) 11709–11715.
[14] A.E. Raevskaya, A.L. Stroyuk, S. Ya. Kuchmii, A.I. Kryukov, Theor. Exp. Chem. 39 (2003) 303–308.
[15] R.A.M. Hikmet, P.T.K. Chin, D.V. Talapin, H. Weller, Adv. Mater. 17 (2005) 1436–1439.
[16] A. Sitt, I. Hadar, U. Banin, Nano Today 8 (2013) 494–513.
[17] K.R. Nemade, S.A. Waghuley, Int. J. Met. 2014 (2014) 389416–389420.
[18] B. Jia, M. Qin, X. Jiang, Z. Zhang, L. Zhang, Y. Liu, X. Qu, J. Nanopart. Res. 15 (2013) 1469–1478.
[19] K. Tezuka, W.C. Sheets, R. Kurihara, Y.J. Shan, H. Imoto, T.J. Marks, K. R. Poeppelmeier, Solid State Sci. 9 (2007) 95–99.
[20] C. Mu, J. He, Nanosc. Res. Lett. 6 (2011) 150–156.
[21] K.R. Nemade, S.A. Waghuley, AIP Conf. Proc. 1536 (2013) 1258–1259.

[22] T. Thomson, B.D. Terris, M.F. Toney, S. Raoux, J.E.E. Baglin, S.L. Lee, S. Sun, J. Appl. Phys. 95 (2004) 6738–6740.
[23] G.Y. Feng, B. Xiao, K. Goerner, G. Cheng, J. Wang, Smart Grid Renew. Energy 2 (2011) 158–164.
[24] B. Minceva-Sukarova, M. Najdoski, I. Grozdanov, C.J. Chunnilall, J. Mol. Struct. 410 (1997) 267–270.
[25] J. Menendez, M. Cardona, Phys. Rev. B 29 (1984) 2051–2059.
[26] H. Tang, I.P. Herman, Phys. Rev. B: Condens. Matter 43 (1991) 2299–2304.
[27] X.L. Yu, C.B. Cao, H.S. Zhu, Q.S. Li, C.L. Liu, Q.H. Gong, Adv. Funct. Mater. 17 (2007) 1397–1401.
[28] J.S. Kim, Y.H. Park, S.M. Kim, J.C. Choi, H.L. Park, Solid State Commun. 133 (2005) 445–448.
[29] J. Ruan, R.J. Xie, N. Hirosaki, T. Takeda, J. Am. Ceram. Soc. 94 (94) (2011) 536–542.
[30] J.W. Li, X.J. Liu, L.W. Yang, Z.F. Zhou, G.F. Xie, Y. Pan, X.H. Wang, J. Zhou, L.T. Li, L. Pan, Z. Sun, C.Q. Sun, Appl. Phys. Lett. 95 (2009) 031906–031909.
[31] K.R. Nemade, S.A. Waghuley, Ceram. Int. 40 (2014) 6109–6113.
[32] K.R. Nemade, S.A. Waghuley, Results Phys. 3 (2013) 52–54.
[33] P.D. Frischmann, K. Mahata, F. Wurthner, Chem. Soc. Rev. 42 (2013) 1847–1870.